Advances in Concrete Construction, *Vol. 9, No. 1* (*2020*) *103-113*
DOI: https://doi.org/10.12989/acc.2020.9.1.103

The effect of nanoparticle in reduction of critical fluid velocity in pipes conveying fluid

M.M. Ghaitani, A. Majidian* and V. Shokri

Department of Mechanical Engineering, Sari Branch, Islamic Azad University, Sari, Iran, P.O.B. 4816119318, Sari, Iran

(*Received October 9, 2019, Revised October 30, 2019, Accepted November 13, 2019*)

Abstract. This paper deal with the critical fluid velocity response of nanocomposite pipe conveying fluid based on numerical method. The pressure of fluid is obtained based on perturbation method. The motion equations are derived based on classical shell theory, energy method and Hamilton's principle. The shell is reinforced by nanoparticles and the distribution of them are functionally graded (FG). The mixture rule is applied for obtaining the equivalent material properties of the structure. Differential quadrature method (DQM) is utilized for solution of the motion equations in order to obtain the critical fluid velocity. The effects of different parameters such asCNT nanoparticles volume percent, boundary conditions, thickness to radius ratios, length to radius ratios and internal fluid are presented on the critical fluid velocity response structure. The results show that with increasing the CNT nanoparticles, the critical fluid velocity is increased. In addition, FGX distribution of nanoparticles is the best choice for reinforcement.

Keywords: critical fluid velocity; pipeline; internal fluid; Differential Quadrature Method

1. Introduction

Fluid-conveying cylindrical pipes have been widely used in many civil and mechanical engineering applications for example in the submarine industry, oil and gas industry, petrochemicals systems, and so on. Such cylindrical structures have been analyzed for many of the failures and/or operating problems due to flow-induced vibrations and instabilities from previous decades (Housner 1952, Benjamin 1961, Païdoussis and Issid 1974).

Several studies have been performed on the dynamical response of the pipes with fluid conveying. Gong *et al*. (2000) applied a computational method for safety evaluation of submerged pipelines, subjected to underwater shock. In this research, the fluid structure interaction between the pipeline and sea water were considered based on the coupled boundary-element and finite-element programs, by means of the Doubly Asymptotic Approximation (DAA). Lee and Oh (2003) developed a spectral element model for the pipe conveying fluid to study the flow induced vibrations of the system by the exact constitutive dynamic stiffness matrix. Lam *et al* (2003) examined the dynamic response of a simply supported laminated underwater pipeline exposed to underwater explosion shock. They concluded that the strength of the radial direction for the pipe is weaker than the strengths in the longitudinal and the circumferential directions. Consequently, the dynamic response of the radial direction is larger than those of other directions. Yoon and Son (2007) studied the dynamic behavior of simply supported fluid-conveying pipe in due to the effect of the open crack and the moving mass. Lin and Qiao (2008) explored vibration and instability of an axially moving beam immersed in fluid with simply supported conditions along with torsional springs. The transient reaction of submerged thin shell subjected to mechanical excitations was studied by Leblond and Sigrist (2010). Huang *et al*. (2010) used Galerkin's method to obtain eigen-frequencies of tubes conveying fluid having different boundary conditions. Further, they calculated the variation of system eigen-frequencies by the effect of the Coriolis forces and expressed a correlation between a pipe conveying fluid and Euler-Bernoulli beam. Zhai *et al*. (2011) used the Timoshenko beam model for obtaining the dynamic response of a fluid-conveying pipe under random excitation. They solved the governing equations by the pseudo excitation method together with complex mode superposition method. Also, they assumed that the parameters of load are random. Liu *et al*. (2012) analyzed fluid-solid interaction problem for an elastic cylinder by numerical simulations and acquired the vibration of cylinder for both laminar and turbulent flows. Dynamic behaviour investigation of pipelines under earthquake acceleration is a research field with few works. Seismic response of natural gas and water pipelines in the Ji-Ji earthquake was considered by Chen *et al*. (2002). They conducted a Statistical analysis for understanding the relationship between seismic factors (the spectrum intensity, peak ground acceleration and peak ground velocity) and repair rates. Also, Abdoun*et al*. (2009) studied influencing factors on the behavior of buried pipelines subjected to earthquake faulting.

In none of mentioned investigations, the structure is not composite. Rationally modeling collapse due to bending and external pressure in pipelines was presented by Nogueira (2012). Effect of using fiber-reinforced polymer

*Corresponding author, Ph.D.
E-mail: a_majidian@iausari.ac.ir

ISSN: 2287-5301 (Print), 2287-531X (Online)

composites for underwater steel pipeline repairs was studied by Shamsuddoha *et al*. (2013). They offered a widespread review about of using fiber-reinforced polymer composites for in-air, underground and underwater pipeline repairs. Ray and Reddy (2013) made a study on the active damping of piezoelectric composite cylindrical shells conveying fluid. The study of composite and nanocomposite plates was presented by Duc *et al*. (2010, 2013, 2014a, 2014b, 2015, 2016, 2018). Chung *et al*. (2013) investigated Polymeric Composite Films Using Modified TiO_2 Nanoparticles. Alijani and Amabili (2014) used energy method with the Amabili-Reddy nonlinear higher-order shear deformation theory for determining the nonlinear vibrations and multiple resonances of fluid filled arbitrary laminated cylindrical shells. They demonstrated that water-filled composite shells may exhibit complex nonlinear dynamic behaviour. Seismic reliability analysis of a jacket-type support structure for an offshore wind turbine was performed by Kim *et al*. (2015). Thinh and Nguyen (2016) investigated the free vibration of composite circular shells containing fluid. They used the Dynamic Stiffness Method (DSM) based on the Reissner-Mindlin theory and non-viscous incompressible fluid equations for modelling of structure. Dynamic characteristic of steady fluid conveying in the periodical partially viscoelastic composite pipeline was studied by Zhou *et al*. (2017). It is shown that the reducing of coverage fraction decreases the flutter velocity. Non-linear vibration of laminated composite circular cylindrical shells using Donnell's shell theory and Incremental Harmonic Balance (IHB) method was analyzed by Dey and Ramachandram (2017). Furthermore, the mechanical behavior of structures containing nanoparticles has been investigated experimentally and analytically by a number of researchers. The influences of nanoparticles on dynamic strength of ultra-high performance was tested by Su *et al*. (2016). Frikha *et al*. (2016) presented a 2-node, 4 DOF/node beam element based on higher order shear deformation theory for axial-flexural-shear functionally graded material. JafarianArani and Kolahchi (2016) studied buckling analysis of columns reinforced with carbon nanotubes by using Euler-Bernoulli and Timoshenko beam models. Buckling of columns retrofitted with Nano-Fiber Reinforced Polymerwas investigated by SafariBilouei *et al*. (2016). Inozemtcev *et al*. (2017) improved the properties of lightweight with hollow microspheres with the nanoscale modifier. Mathematical modeling of pipes reinforced with CNTs conveying fluid for vibration and stability analysis was done by Zamani Nouri (2017). Vibration of Silica nanoparticles-reinforced beams considering agglomeration effects was considered by Shokravi (2017). Also, RabaniBidgoli and Saeidifar (2017) studied time-dependent buckling of CNT nanoparticles reinforced columns exposed to fire. A hybrid pipe-shell element based numerical model programed by INP code supported by ABAQUS solver was proposed by Liu *et al*. (2017) to explore the strain performance of buried X80 steel pipeline under reverse fault displacement. Recently, Seismic response of CNT nanoparticles-reinforced surface pipes was investigated by Motezaker and Kolahchi (2017). In this research, the pipes were unsubmerged. Dynamic response of the horizontal

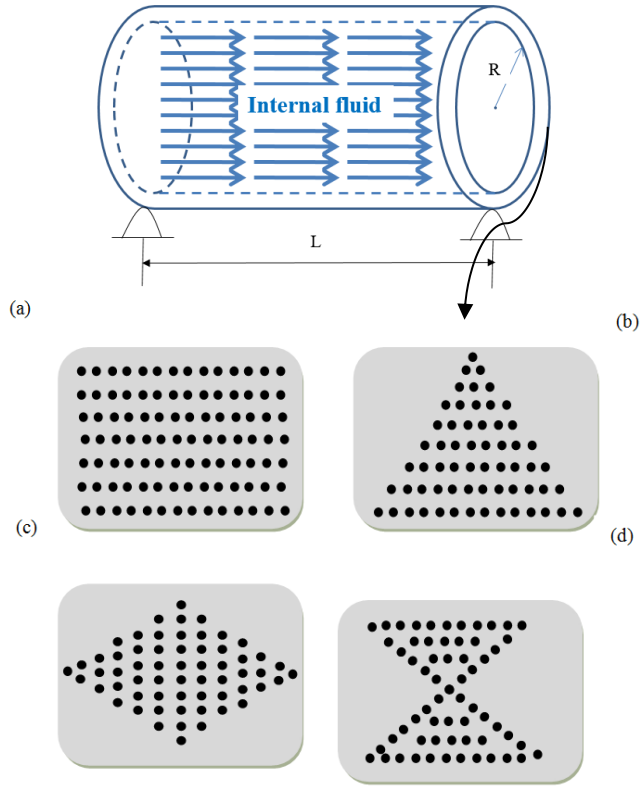

Fig. 1 Schematic of nanocomposite pipe conveying fluid

beam subjected to seismic ground excitation was investigated by Mohammadian *et al*. (2017). Non-linear dynamics analysis of functionally graded material (FGM) shell structures was investigated by Hajlaoui *et al*. (2017) using the higher order solid-shell element based on the Enhanced Assumed Strain (EAS). Vibration and nonlinear dynamic response of eccentrically stiffened functionally graded composite truncated conical shells in thermal environments were presented by Chan *et al*. (2018). Nonlinear response and buckling analysis of eccentrically stiffened FGM toroidal shell segments in thermal environment were studied vy Vuong and Duc (2018). Sharifi *et al*. (2018) studied the dynamic analysis of a column reinforced with titanium dioxide (TiO2) nanoparticles under earthquake load. Hajlaoui *et al*. (2019a) presented a modified first-order enhanced solid-shell element formulation with an imposed parabolic shear strain distribution through the shell thickness in the compatible strain part. Hajlaoui *et al*. (2019b) investigated buckling behaviors of functionally graded carbon nanotube-reinforced composites (FG-CNTRC) shells using a modified first-order enhanced solid-shell element formulation. Static behavior of carbon nanotubes (CNTs) reinforced functionally graded shells using an efficient solid-shell element with parabolic transverse shear strain was studied by Hajlaoui *et al*. (2019c).

Hitherto, the dynamic behavior of the nanocomposite pipes conveying fluid has not been investigated by any researcher. So in this research, for the first time, the critical fluid velocity response of the nanocomposite pipe conveying fluid is analytically considered as the importance

of the subject. Mixture method is used to evaluate the material properties of the nanocomposite. The governing equations of the structure are derived using energy method and according to classical theory. The critical fluid velocity of the structure is derived using differential quadrature method (DQM). In present study, effect of various parameters like volume percent of CNTs, boundary conditions, geometrical parameters of pipe, internal fluid on the critical fluid velocity of the structure is presented.

2. Mathematical modeling

As shown in Fig. 1, a nanocomposite cylindrical pipe conveying fluid with length a, radius R and thickness h is considered.

2.1 Strain-displacement relationships

In order to calculate the middle-surface strain and curvatures, using Kirchhoff-Law assumptions, the displacement components of cylindrical shell in the axial x, circumferential θ, and radial z directions can be written as (Brush and Almroth 1975)

$$u_1(x,\theta,z,t)=u(x,\theta,t)-z\frac{\partial w(x,\theta,t)}{\partial x}, \tag{1a}$$

$$u_2(x,\theta,z,t)=v(x,\theta,t)-\frac{z}{R}\frac{\partial w(x,\theta,t)}{\partial \theta}, \tag{1b}$$

$$u_3(x,\theta,z,t)=w(x,\theta,t), \tag{1c}$$

where (u_1, u_2, u_3) denotes the displacement components at an arbitrary point (x,θ,z) in the shell, and (u,v,w) are the displacement components of the middle surface of the shell in the axial, circumferential and radial directions, respectively. Also, z is the distance from an arbitrary point to the middle surface. Using Donnell's linear theory and applying Eqs. (1)-(3), strain-displacement relationships may be written as

$$\varepsilon_{xx}=\frac{\partial u}{\partial x}-z\frac{\partial^2 w}{\partial x^2}, \tag{2a}$$

$$\varepsilon_{\theta\theta}=\frac{\partial v}{R\partial\theta}+\frac{w}{R}-\frac{z}{R^2}\frac{\partial^2 w}{\partial\theta^2}, \tag{2b}$$

$$\varepsilon_{xy}=\frac{1}{2}\left(\frac{\partial u}{R\partial\theta}+\frac{\partial v}{\partial x}\right)-z\frac{\partial^2 w}{R\partial x\partial\theta}, \tag{2c}$$

where (ε_{xx}, $\varepsilon_{\theta\theta}$) are the normal strain components and ($\varepsilon_{x\theta}$) is the shear strain component.

The constitutive equation for stresses σ and strains ε matrix may be written as follows

$$\begin{bmatrix}\sigma_{xx}\\ \sigma_{\theta\theta}\\ \tau_{x\theta}\end{bmatrix}=\begin{bmatrix}C_{11} & C_{12} & 0\\ C_{21} & C_{22} & 0\\ 0 & 0 & C_{66}\end{bmatrix}\begin{bmatrix}\varepsilon_{xx}\\ \varepsilon_{\theta\theta}\\ \gamma_{x\theta}\end{bmatrix}, \tag{3}$$

2.2 Mixture rule

According to this theory, the effective Young and shear moduli of structure may be expressed as (Liew 2014, Zhang 2015h)

$$E_{11}=\eta_1 V_{CNT}E_{r11}+(1-V_{CNT})E_m, \tag{4a}$$

$$\frac{\eta_2}{E_{22}}=\frac{V_{CNT}}{E_{r22}}+\frac{(1-V_{CNT})}{E_m}, \tag{4b}$$

$$\frac{\eta_3}{G_{12}}=\frac{V_{CNT}}{G_{r12}}+\frac{(1-V_{CNT})}{G_m}, \tag{4c}$$

where E_{r11}, E_{r22} and E_m are Young's moduli of CNTs and matrix, respectively; G_{r11} and G_m are shear modulus of CNTs and matrix, respectively; V_{CNT} and V_m show the volume fractions of the CNTs and matrix, respectively; η_j (j=1, 2, 3) is CNT efficiency parameter for considering the size-dependent material properties. Noted that this parameter may be calculated using molecular dynamic (MD). However, the CNT distribution for the mentioned patters obeys from the following relations (Zhang 2015h, Liew *et al*. 2014)

$$UD:\ V_{CNT}=V_{CNT}^*, \tag{5a}$$

$$FGV:\ V_{CNT}(z)=\left(1+\frac{2z}{h}\right)V_{CNT}^*, \tag{5b}$$

$$FGO:\ V_{CNT}(z)=2\left(1-\frac{2|z|}{h}\right)V_{CNT}^*, \tag{5c}$$

$$FGX:\ V_{CNT}(z)=2\left(\frac{2|z|}{h}\right)V_{CNT}^*, \tag{5d}$$

Furthermore, the thermal expansion coefficients in the axial and transverse directions respectively (α_{11} and α_{22}) and the density (ρ) of the nano-composite structure can be written as (Liew *et al*. 2014)

$$\rho=V_{CNT}\rho_r+V_{m,}\rho_{m,}, \tag{6}$$

$$\alpha_{11}=V_{CNT}\alpha_{r11}+V_{m,}\alpha_{m,}, \tag{7}$$

$$\alpha_{22}=(1+\nu_{r12})V_{CNT}\alpha_{r22}+(1+\nu_m)V_m\alpha_m-\nu_{12}\alpha_{11}, \tag{8}$$

where

$$V_{CNT}^*=\frac{w_{CNT}}{w_{CNT}+(\rho_{CNT}/\rho_m)-(\rho_{CNT}/\rho_m)w_{CNT}}, \tag{9}$$

where w_{CNT} is the mass fraction of the CNT; ρ_m and ρ_{CNT} present the densities of the matrix and CNT, respectively; ν_{r12} and ν_m are Poisson's ratios of the CNT and matrix, respectively; α_{r11}, α_{r22} and α_m are the thermal expansion coefficients of the CNT and matrix, respectively. Noted that ν_{12} is assumed as constant.

3. Motion equations

In this part, the governing equation of motion can be

obtained using energy method.

3.1 Energy method

The total potential energy, V, of the cylindrical shell conveying fluid is the sum of strain energy U, kinetic energy K, and the work done by the fluid W.

The strain energy can be written as

$$U = \int_V \left(\sigma_{xx}\varepsilon_{xx} + \sigma_{\theta\theta}\varepsilon_{\theta\theta} + \sigma_{x\theta}\gamma_{x\theta}\right) dV, \tag{10}$$

By substituting Eqs. (4)- (6) into (10) yields

$$\begin{aligned} U = \int_{-\frac{h}{2}}^{\frac{h}{2}} \iint_A \Bigg(& \sigma_x \left(\frac{\partial u}{\partial x} + 0.5\left(\frac{\partial w}{\partial x}\right)^2 - z\frac{\partial^2 w}{\partial x^2} \right) \\ & + \sigma_\theta \left(\frac{\partial v}{R\partial\theta} + \frac{w}{R} + 0.5\left(\frac{\partial w}{R\partial\theta}\right)^2 - z\frac{\partial^2 w}{R^2\partial\theta^2} \right) \\ & + \sigma_{x\theta} \left(\frac{\partial u}{R\partial\theta} + \frac{\partial v}{\partial x} + \frac{\partial w}{R\partial\theta}\frac{\partial w}{\partial x} - 2z\frac{\partial^2 w}{R\partial\theta\partial x} \right) \Bigg) dz\, dA \end{aligned} \tag{11}$$

By introducing force and moment resultants as Eqs. (12)-)13) and substituting in Eq. (11), Eq. (14) yields

$$\begin{Bmatrix} N_x \\ N_\theta \\ N_{x\theta} \end{Bmatrix} = \int_{-\frac{h}{2}}^{\frac{h}{2}} \begin{Bmatrix} \sigma_x \\ \sigma_\theta \\ \tau_{x\theta} \end{Bmatrix} dz, \tag{12}$$

$$\begin{Bmatrix} M_x \\ M_\theta \\ M_{x\theta} \end{Bmatrix} = \int_{-\frac{h}{2}}^{\frac{h}{2}} \begin{Bmatrix} \sigma_x \\ \sigma_\theta \\ \tau_{x\theta} \end{Bmatrix} z dz, \tag{13}$$

$$\begin{aligned} U = \int_A \Bigg(& N_x \left(\frac{\partial u}{\partial x} + 0.5\left(\frac{\partial w}{\partial x}\right)^2 \right) - M_x \frac{\partial^2 w}{\partial x^2} \\ & + N_\theta \left(\frac{\partial v}{R\partial\theta} + \frac{w}{R} + 0.5\left(\frac{\partial w}{R\partial\theta}\right)^2 \right) \\ & - M_\theta \frac{\partial^2 w}{R^2\partial\theta^2} + N_{x\theta}\left(\frac{\partial u}{R\partial\theta} + \frac{\partial v}{\partial x} + \frac{\partial w}{R\partial\theta}\frac{\partial w}{\partial x} \right) \\ & - 2M_{x\theta}\frac{\partial^2 w}{R\partial\theta\partial x} \Bigg) dA \end{aligned} \tag{14}$$

The kinetic energy may be expressed as

$$K = \frac{\rho}{2}\int_v \left(\left(\frac{\partial u_1}{\partial t}\right)^2 + \left(\frac{\partial u_2}{\partial t}\right)^2 + \left(\frac{\partial u_3}{\partial t}\right)^2 \right) dV, \tag{15}$$

By substituting Eqs. (1)-(3) into (15) and defining the following term

$$\begin{Bmatrix} h \\ 0 \\ \frac{h^3}{12} \end{Bmatrix} = \int_{-h/2}^{h/2} \begin{bmatrix} 1 \\ z \\ z^2 \end{bmatrix} dz, \tag{16}$$

We have

$$\begin{aligned} K = \int \Bigg(& \frac{\rho}{2}\left(\frac{h^3}{12}\left(\left(\frac{\partial^2 u}{\partial t\,\partial x}\right)^2 + \left(\frac{\partial^2 w}{\partial t\partial\theta}\right)^2 \right) \right. \\ & \left. + h\left(\left(\frac{\partial u}{\partial t}\right)^2 + \left(\frac{\partial v}{\partial t}\right)^2 + \left(\frac{\partial w}{\partial t}\right)^2 \right) \right) dA. \end{aligned} \tag{17}$$

The fluid structure interaction is described by linear potential flow theory. The flow velocity $\boldsymbol{V}$ may be expressed as (Amabili *et al*. 2008)

$$\boldsymbol{V} = -\nabla\Psi, \tag{18}$$

where ψ is a potential function including two components due to mean undisturbed flow velocity v_x and the shell motions. Hence

$$\Psi = -v_x x + \Phi, \tag{19}$$

The potential of the unsteady component Φ satisfies the Laplace equation

$$\nabla^2\Phi = \frac{\partial^2\Phi}{\partial x^2} + \frac{\partial^2\Phi}{\partial r^2} + \frac{1}{r}\frac{\partial\Phi}{\partial r} + \frac{1}{r^2}\frac{\partial\Phi}{\partial\theta^2} = 0, \tag{20}$$

In order to obtain the perturbed pressure (P) in term of velocity potential, the Bernoulli's equation is used as

$$-\frac{\partial\Phi}{\partial t} + \frac{1}{2}V^2 + \frac{\bar{P} + p}{\rho_e} = \frac{\bar{P} + 1/2\rho_f (v_x)^2}{\rho_e}, \tag{21}$$

where $\bar{P}$ and p are the mean pressure and perturbation pressure, respectively and for small perturbations we have

$$V^2 = (v_x)^2 - 2v_x\frac{\partial\Phi}{\partial x}, \tag{22}$$

However, combining Eqs. (21) and (22) yields the perturbation pressure as follows

$$p = \rho_e\left(\frac{\partial\Phi}{\partial t} + v_x\frac{\partial\Phi}{\partial x} \right) \tag{23}$$

Assuming that there is no cavitation at the fluid-pipe interface, the boundary condition between the pipe wall and the flow is

$$\left(\frac{\partial\Phi}{\partial r}\right)_{r=R} = \left(\frac{\partial w}{\partial t} + v_x\frac{\partial w}{\partial x} \right), \tag{24}$$

in which w is the transverse deflection of the structure. Using the method of variables separation for Φ, we have

$$\Phi(\mathrm{x},\mathrm{r},\theta,\mathrm{t}) = \sum_{m=1}^{M}\sum_{n=0}^{N} \Phi_m(\mathrm{x})\psi_{m,n}(\mathrm{r})\cos(\mathrm{n}\,\theta)\,\mathrm{f}_{m,n}(\mathrm{t}), \tag{25}$$

Substituting Eq. (38) into Eq. (33) and assuming regularity condition at r=0 for the for potential of perturbation velocity yields

$$\begin{aligned} \Phi_m &= \sin\left(\frac{m\pi x}{L}\right), \\ \psi_{m,n}(\mathrm{r}) &= I_n\left(\frac{m\pi r}{L}\right), \end{aligned} \tag{26}$$

where I_n is the first kind modified Bessel function in the order of n. Combining Eqs. (25) and (26) yields

$$\Phi(\mathrm{x},\mathrm{r},\theta,\mathrm{t})=\sum_{m=1}^{M}\sum_{n=0}^{N}\frac{L}{m\pi}\frac{I_n(m\pi r/L)}{I_n^{'}(m\pi R/L)}\left(\frac{\partial w}{\partial t}+v_x\frac{\partial w}{\partial x}\right), \quad (27)$$

in which I'_n is first derivative of I_n.

3.2 Hamilton's principle

The governing equations of the structure are derived using the Hamilton's principle which is considered as follows

$$\int_0^t(\delta U-\delta K)dt=0. \quad (28)$$

Now, by applying the Hamilton's principle and after integration by part and some algebraic manipulation, three equations of motion can be derived as follows

$$\frac{\partial N_x}{\partial x}+\frac{\partial N_{x\theta}}{R\partial\theta}=\rho h\frac{\partial^2 u}{\partial t^2}, \quad (29)$$

$$\frac{\partial N_\theta}{R\partial\theta}+\frac{\partial N_{x\theta}}{\partial x}=\rho h\frac{\partial^2 v}{\partial t^2}, \quad (30)$$

$$\begin{aligned}&\frac{\partial^2 M_x}{\partial x^2}+\frac{2\partial^2 M_{x\theta}}{R\,\partial x\,\partial\theta}+\frac{\partial^2 M_\theta}{R^2\partial\theta^2}-\frac{N_\theta}{R}+N_x\frac{\partial^2 w}{\partial x^2}+N_\theta\frac{\partial^2 w}{R^2\partial\theta^2}\\&+N_{x\theta}\frac{2\partial^2 w}{R\partial x\,\partial\theta}+\rho_e\left(\frac{\partial\Phi}{\partial t}+v_x\frac{\partial\Phi}{\partial x}\right)=\rho h\frac{\partial^2 w}{\partial t^2},\end{aligned} \quad (31)$$

By integrating the stress-strain relations of the structure and introduced Eqs. (12)-(13), we have

$$N_x=h\left(C_{11}\left(\frac{\partial u}{\partial x}+0.5\left(\frac{\partial w}{\partial x}\right)^2\right)+C_{12}\left(\frac{\partial v}{R\partial\theta}+\frac{w}{R}+0.5\left(\frac{\partial w}{R\partial\theta}\right)^2\right)\right), \quad (32)$$

$$N_\theta=h\left(C_{12}\left(\frac{\partial u}{\partial x}+0.5\left(\frac{\partial w}{\partial x}\right)^2\right)+C_{22}\left(\frac{\partial v}{R\partial\theta}+\frac{w}{R}+0.5\left(\frac{\partial w}{R\partial\theta}\right)^2\right)\right), \quad (33)$$

$$N_{x\theta}=h\left(C_{66}\left(\frac{\partial u}{R\partial\theta}+\frac{\partial v}{\partial x}+\frac{\partial w}{R\partial\theta}\frac{\partial w}{\partial x}\right)\right), \quad (34)$$

$$M_x=\frac{h^3}{12}\left(C_{11}\left(-z\frac{\partial^2 w}{\partial x^2}\right)+C_{12}\left(-z\frac{\partial^2 w}{R^2\partial\theta^2}\right)\right), \quad (35)$$

$$M_\theta=\frac{h^3}{12}\left(C_{12}\left(-z\frac{\partial^2 w}{\partial x^2{}_x}\right)+C_{22}\left(-z\frac{\partial^2 w}{R^2\partial\theta^2}\right)\right), \quad (36)$$

$$M_{x\theta}=\frac{h^3}{12}C_{66}\left(-2z\frac{\partial^2 w}{R\partial\theta\partial x}\right). \quad (37)$$

By substituting stress resultants, Eqs. (32)-(37), in governing equations, Eqs. (29)-(31), relations can be obtained in terms of only the displacement fields.

Also, the boundary conditions are taken into account as below

Clamped-Clamped supported

$$\begin{aligned}&w=v=u=0 \qquad @\quad x=0,L\\&\frac{\partial w}{\partial x}=0 \qquad @\quad x=0,L\end{aligned} \quad (38)$$

Simply-Simply supported

$$\begin{aligned}&w=v=\frac{\partial^2 w}{\partial x^2}=0 \qquad @\quad x=0\\&w=v=\frac{\partial^2 w}{\partial x^2}=0 \qquad @\quad x=L\end{aligned} \quad (39)$$

Clamped-Simply supported

$$\begin{aligned}&w=v=u=\frac{\partial w}{\partial x}=0 \qquad @\quad x=0\\&w=v=\frac{\partial^2 w}{\partial x^2}=0 \qquad @\quad x=L\end{aligned} \quad (40)$$

3.3 DQ method

In recent years, the method of DQ has become increasingly popular in the numerical solution of problems in analysis of structural and dynamical problems. In these method, the derivative of the function may be defined as follows (Kolahchi *et al*. 2015)

$$\frac{d^n f_x(x_i,\theta_j)}{dx^n}=\sum_{k=1}^{N_x}A_{ik}^{(n)}f(x_k,\theta_j) \qquad n=1,...,N_x-1. \quad (41)$$

$$\frac{d^m f_y(x_i,\theta_j)}{d\theta^m}=\sum_{l=1}^{N_\theta}B_{jl}^{(m)}f(x_i,\theta_l) \qquad m=1,...,N_\theta-1. \quad (42)$$

$$\frac{d^{n+m}f_{xy}(x_i,\theta_j)}{dx^n d\theta^m}=\sum_{k=1}^{N_x}\sum_{l=1}^{N_\theta}A_{ik}^{(n)}B_{jl}^{(m)}f(x_k,\theta_l). \quad (43)$$

where N_x and N_θ denote the number of points in x and θdirections, $f(x,\theta)$ is the function, and A_{ik}, B_{jl} are the weighting coefficients defined as

$$A_{ij}^{(1)}=\begin{cases}\dfrac{M(x_i)}{(x_i-x_j)M(x_j)} & for \quad i\neq j,\quad i,j=1,2,...,N_x\\ -\sum\limits_{\substack{j=1\\ i\neq j}}^{N_x}A_{ij}^{(1)} & for \quad i=j,\quad i,j=1,2,...,N_x\end{cases} \quad (44)$$

$$B_{ij}^{(1)}=\begin{cases}\dfrac{P(\theta_i)}{(\theta_i-\theta_j)P(\theta_j)} & for \quad i\neq j,\quad i,j=1,2,...,N_\theta,\\ -\sum\limits_{\substack{j=1\\ i\neq j}}^{N_\theta}B_{ij}^{(1)} & for \quad i=j,\quad i,j=1,2,...,N_\theta\end{cases} \quad (45)$$

where M and P are Lagrangian operators defined as

$$M(x_i)=\prod_{\substack{j=1\\ j\neq i}}^{N_x}(x_i-x_j) \quad (46)$$

$$P(\theta_i)=\prod_{\substack{j=1\\ j\neq i}}^{N_\theta}(\theta_i-\theta_j) \quad (47)$$

and for higher-order derivatives, we have

$$A_{ij}^{(n)}=n\left(A_{ii}^{(n-1)}A_{ij}^{(1)}-\frac{A_{ij}^{(n-1)}}{(x_i-x_j)}\right) \quad (48)$$

$$B_{ij}^{(m)} = m\left(B_{ii}^{(m-1)}B_{ij}^{(1)} - \frac{B_{ij}^{(m-1)}}{(\theta_i - \theta_j)}\right) \quad (49)$$

The Chebyshev polynomialsare used as below for selecting sampling grid points

$$X_i = \frac{L}{2}\left[1-\cos\left(\frac{i-1}{N_x-1}\right)\pi\right] \quad i=1,...,N_x \quad (50)$$

$$\theta_i = \frac{2\pi}{2}\left[1-\cos\left(\frac{i-1}{N_\theta-1}\right)\pi\right] \quad i=1,...,N_\theta \quad (51)$$

Assuming Eqs. (52)-(54) (for changing relations to standard eigenvalue problem form) and applying above equations into the motion equations, the matrix form of governing equations can be written as Eq. (53)

$$\bar{u}(x,y,t) = \bar{u}(x,y)e^{\lambda\tilde{t}}, \quad (52)$$

$$\bar{v}(x,y,t) = \bar{v}(x,y)e^{\lambda\tilde{t}}, \quad (53)$$

$$\bar{w}(x,y,t) = \bar{w}(x,y)e^{\lambda\tilde{t}}, \quad (54)$$

$$\left(\underbrace{\left[K_L + K_{NL}\right]}_{K} + \Omega[C] + \Omega^2[M]\right)\begin{Bmatrix}\{d_b\}\\ \{d_d\}\end{Bmatrix} = \begin{Bmatrix}\{0\}\\ \{0\}\end{Bmatrix}, \quad (55)$$

where K_L, K_{NL}, C, M, d_b and d_d represent the linear stiffness matrix, the nonlinear stiffness matrix, the damping matrix, the mass matrix, the boundary points and domain points, respectively. Finally, based on eigenvalue problem, the critical fluid velocity can be obtained.

4. Numerical results and discussion

A computer program based on the DQM being written in MATLAB to solve the nonlinear motion equations. It is assumed the flowing liquid is water. The mass density of water is equal to (9982 Kg/m^3) and (10^{-3} Pas) respectively. Poly methyl methacrylate (PMMA) is selected for the matrix which have constant Poisson's ratios of v_m=0.34, and Young moduli of E_m=3.52 GPa. In addition, CNTs have the density of ρ_{CNT}=6700 Kg/m^3, elastic constants of $E_{11}^{CNT} = 5.6466\,(\text{TPa})$, $E_{22}^{CNT} = 7.080\,(\text{TPa})$ and $G_{12}^{CNT} = 1.9445\,(\text{TPa})$. Furthermore, the cylindrical shell is investigated with three kinds of boundary conditions: two edges simply supported (SS), clamped (CC), and simply supported and clamped (SC).

4.1 Validation

In order to show the accuracy of the present work, neglecting the CNTs and fluid, the results are compared with the work of Amabili (2008). However, considering a pipe with elastic mudulus of E=206 GPa, Poisson's ratio of v=0.3, density ρ=7850 Kg/m^3, length to radius ration of L/R=2 and thickness to radius ration of h/R=0.01, the dimensionless frequency ($\Omega = \omega / \left\{\pi^2 / L^2\left[D/\rho h\right]\right\}^{0.5}$) is plotted versus dimensionless fluid velocity ($V = v_x / \left\{\pi^2 / L\left[D/\rho h\right]\right\}^{0.5}$) in Fig. 2. As can be seen, present results are agree well with the results of Amabili (2008).

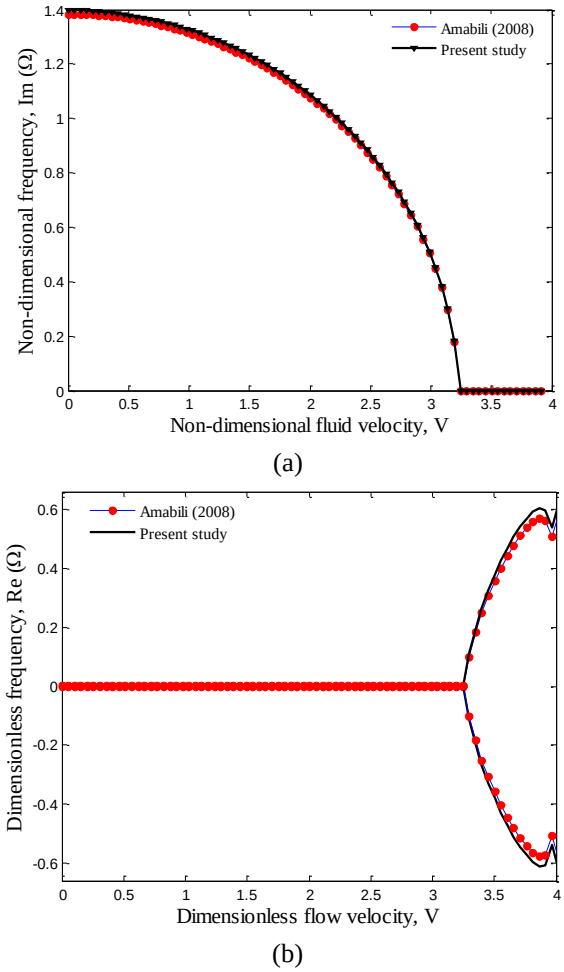

Fig. 2 Validation of present work (a) frequency (b) damping

4.1 The convergence of present method

Fig. 3 shows the effect of DQ point number on the dimensionless natural frequency ($\text{Im}(\Omega = \omega R\sqrt{\rho/E})$) and damping ($\text{Re}(\Omega)$) of pipe versus dimensionless flow velocity ($V = \sqrt{\rho_f / C_{11}}\, v_x$), respectively. As can be seen, $\text{Im}(\Omega)$ decreases with increasing V, while the $\text{Re}(\Omega)$ remains zero. These imply that the system is stable. When the natural frequency becomes zero, critical velocity is reached, which the system loses its stability due to the divergence via a pitchfork bifurcation. Hence, the eigen-frequencies have the positive real parts, which the system becomes unstable. In this state, both real and imaginary parts of frequency become zero at the same point. Therefore, with increasing flow velocity, system stability decreases and became susceptible to buckling. It can be seen that the dimensionless frequency is decreased with increasing the grid point number and for N=17, the results become converge.

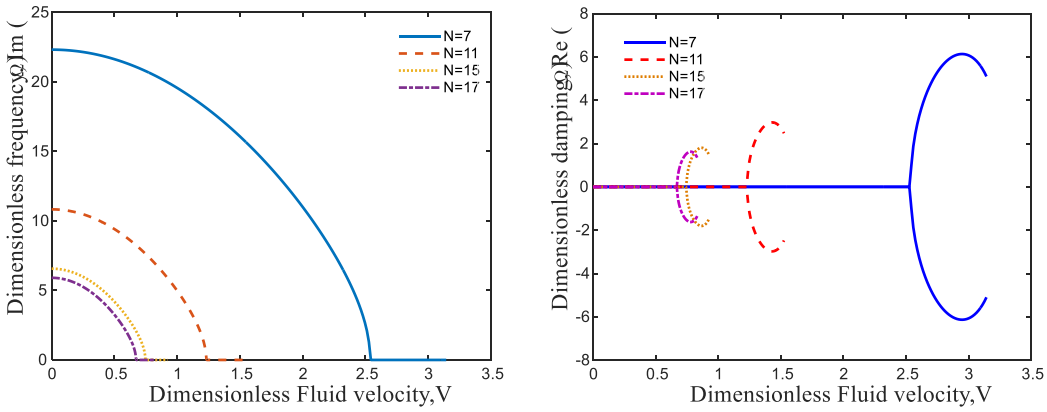

Fig. 3 Convergence of present solution method (a) frequency (b) damping

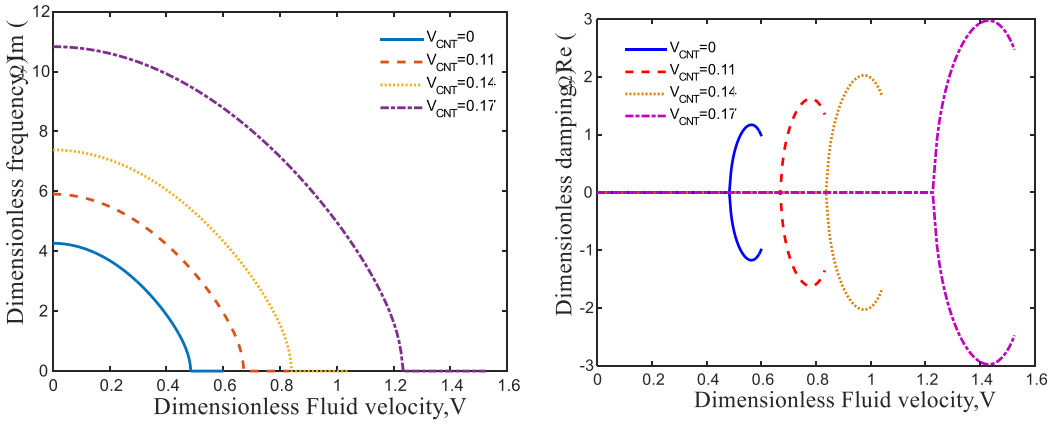

Fig. 4 The effect of CNT nanoparticles on the (a) frequency (b) damping

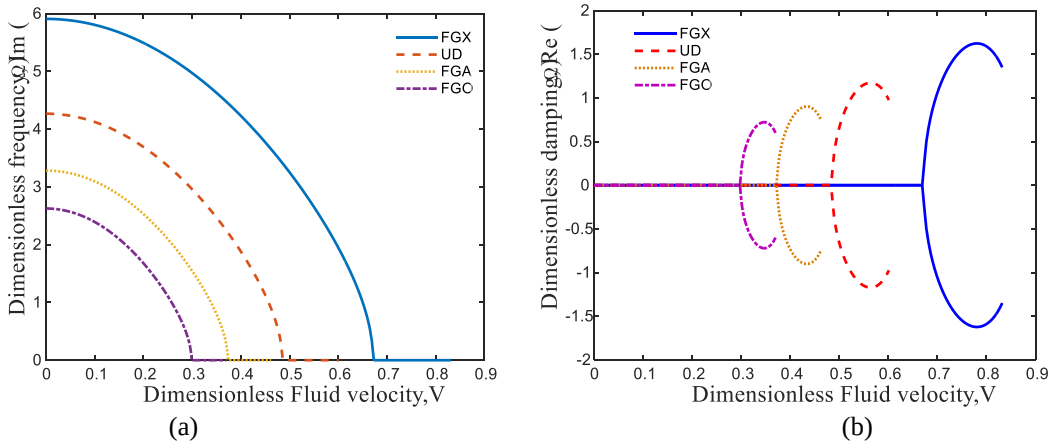

Fig. 5 The effect of CNT nanoparticles distribution type on the (a) frequency (b) damping

4.3 Effect of various parameters

Fig. 4 illustrates the effect of nanoparticles volume percent on the dimensionless frequency and damping of the structure. A direct relationship can be fine between nanoparticles volume percent and frequency of the structure so that with increasing the nanoparticles volume percent, the dimensionless frequency and critical fluid velocity is increased. It is because with increasing the nanoparticles volume percent, the fluid velocity which leads to instability educes.

Depicted in Fig. 5 is the non-dimensional frequency and damping for the UD and three types of FG distributions of nanoparticles versus dimensionless flow velocity. As can be seen, the frequency and critical fluid velocity of FGA- and FGO- CNTRC cylindrical shell are smaller than those of UD-CNTRC cylindrical shell while the FGX- CNTRC cylindrical shell has higher frequency and critical fluid

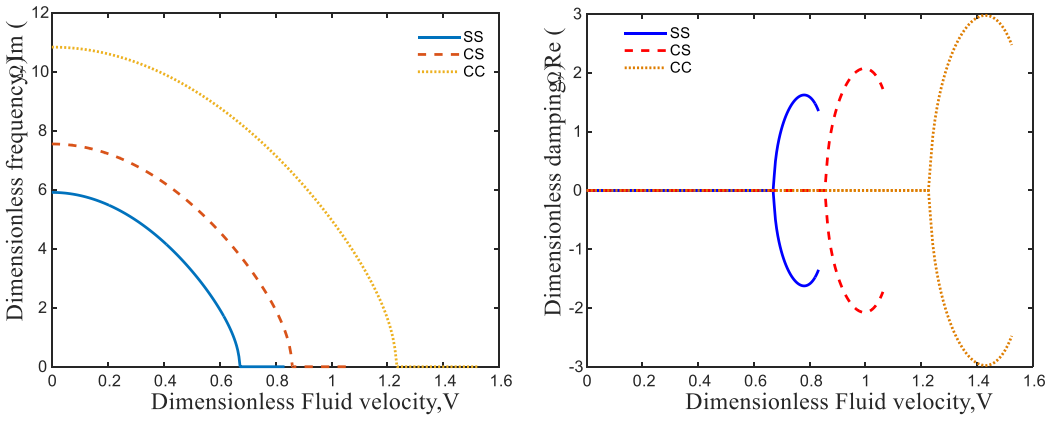

(a) (b)

Fig. 6 The effect of boundary conditions on the (a) frequency (b) damping

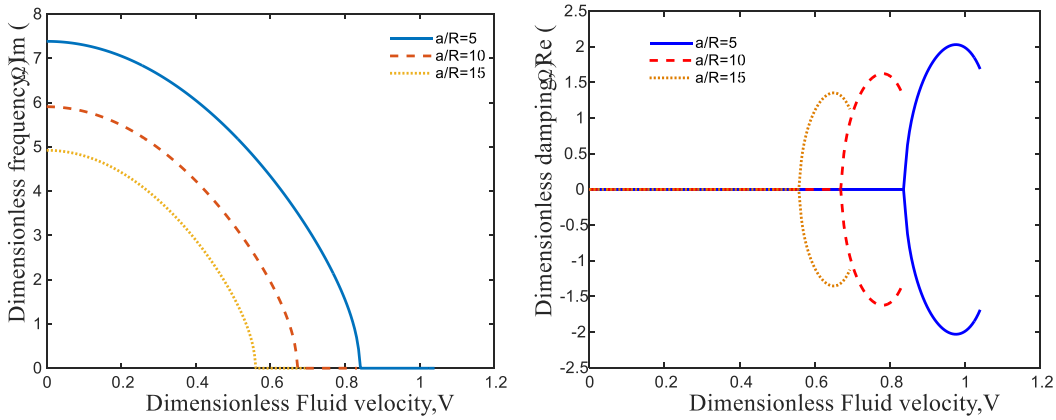

(a) (b)

Fig. 7 The effect of length to radius ratio of pipe on the (a) frequency (b) damping

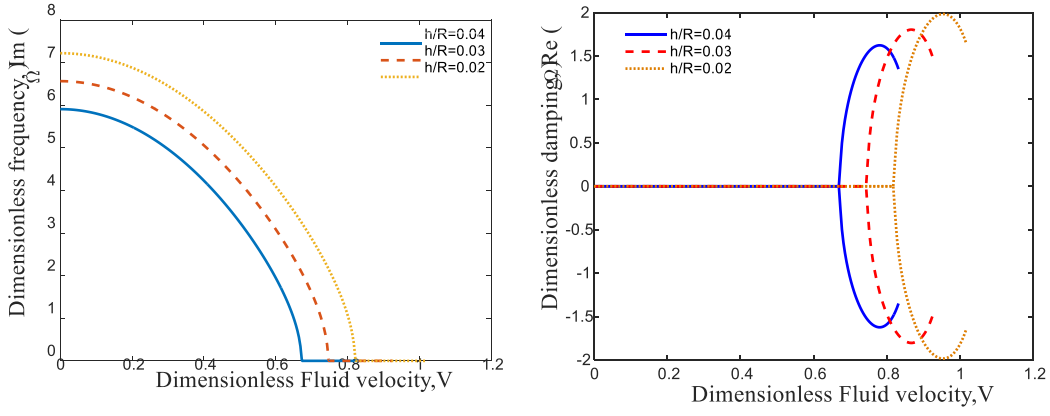

(a) (b)

Fig. 8 The effect of thickness to radius ratio of pipe on the (a) frequency (b) damping

velocity with respect to three other cases. It is due to the fact that the stiffness of CNTRC cylindrical shell changes with the form of CNT distribution in matrix. However, it can be concluded that CNT distribution close to top and bottom are more efficient than those distributed nearby the mid-plane for increasing the stiffness of plates.

Fig. 6 presents the effect of different boundary condition on the dimensionless frequency and damping of the pipe versus the dimensionless fluid velocity. It can be observed that the clamped-clamped (CC) boundary condition leads to higher dimensionless frequency and critical fluid velocity with respect to other considered boundary conditions. It is due to the fact that the cylindrical shell with CC boundary condition has higher bending rigidity.

Fig. 7 demonstrates the effect of length to radius ratio of the cylindrical shell on the dimensionless frequency and damping of the pipe against the dimensionless fluid velocity. As can be seen, with increasing the length to

radius ratio of the cylindrical shell, the dimensionless frequency and critical fluid velocity are decreased due to reduction in the stiffness of the structure.

Fig. 8 presents the effect of thickness to radius ratio of the cylindrical shell on the dimensionless frequency and damping of the pipe against the dimensionless fluid velocity. As can be seen, with increasing the thickness to radius ratio of the cylindrical shell, the dimensionless frequency and critical fluid velocity are enhanced due to increase in the stiffness of the structure.

5. Conclusions

The critical fluid velocity response of nanocomposite pipeline conveying fluid was investigated in this study. The nanotechnology was used for improving the mechanical behavior of pipe and it was strengthened with CNT nanoparticles. The mixture rule was applied for determining the elastic coefficients of nanocomposite assuming FG distribution for nanoparticles. Perturbation equation was employed to calculate the internal fluid effect in the pipe. The motion equations were derived using an energy method and Hamilton's principle and solved via DQM. The effects of boundary conditions, volume percent of CNT nanoparticles, geometrical parameters of pipe and the fluid on the critical fluid velocity of the structure were taken into considerations. Results indicate:

1-With increasing the nanoparticles volume percent, the dimensionless frequency and critical fluid velocity was increased..

2-The frequency and critical fluid velocity of FGA- and FGO- CNTRC cylindrical shell were smaller than those of UD-CNTRC cylindrical shell while the FGX-CNTRC cylindrical shell has higher frequency and critical fluid velocity with respect to three other cases.

3-It can be observed that the clamped-clamped (CC) boundary condition leads to higher dimensionless frequency and critical fluid velocity with respect to other considered boundary conditions.

4-With increasing the length to radius ratio of the cylindrical shell, the dimensionless frequency and critical fluid velocity were decreased due to reduction in the stiffness of the structure.

5-With increasing the thickness to radius ratio of the cylindrical shell, the dimensionless frequency and critical fluid velocity were enhanced due to increase in the stiffness of the structure.

References

Abdoun, T.H., Ha, D., O'Rourke, M., Symans, M., O'Rourke, T., Palmer, M. and Harry, E. (2009), "Factors influencing the behavior of buried pipelines subjected to earthquake faulting", *Soil Dyn. Earthq. Eng.*, **29**, 415-427. https://doi.org/10.1016/j.soildyn.2008.04.006.

Alijani, F. and Amabili, M. (2014), "Nonlinear vibrations and multiple resonances of fluid filled arbitrary laminated circular cylindrical shells", *Compos. Struct.*, **108**, 951-962. https://doi.org/10.1016/j.compstruct.2013.10.029.

Amabili, M. (2008), *Nonlinear Vibrations and Stability of Shells and Plates*, Cambridge University Press, Cambridge.

Benjamin, T.B. (1961), "Dynamics of a system of articulated pipes conveying fluid", *Proc. Royal Soc. A.*, **261**(130), 457-486. https://doi.org/10.1098/rspa.1961.0090.

Brush, O. and Almorth, B. (1975), *Buckling of Bars, Plates and Shells*, Mc-Graw Hill.

Chan, D.Q., Anh, V.T.T. and Duc, N.D. (2018), "Vibration and nonlinear dynamic response of eccentrically stiffened functionally graded composite truncated conical shells in thermal environments", *Acta Mech.*, **230**, 157-178. https://doi.org/10.1007/s00707-018-2282-4.

Chen, W., Shih, B.J., Chen, Y.C., Hung, J.H. and Hwang, H.H. (2002), "Seismic response of natural gas and water pipelines in the Ji-Ji earthquake", *Soil Dyn. Earthq. Eng.*, **22**, 1209-1214. https://doi.org/10.1016/S0267-7261(02)00149-5.

Chung, D.N., Dinh, N.N., Hui, D., Duc, N.D., Trung, T.Q. and Chipara, M. (2013), "Investigation of polymeric composite films using modified TiO_2 nanoparticles for organic light emitting diodes", *J. Current Nanosci.*, **9**, 14-20. https://doi.org/10.2174/157341313805118018.

Dey, T. and Ramachandra, L.S. (2017), "Non-linear vibration analysis of laminated composite circular cylindrical shells", *Compos. Struct.*, **163**, 89-100. https://doi.org/10.1016/j.compstruct.2016.12.018.

Duc, N.D. (2014a), *Nonlinear Static and Dynamic Stability of Functionally Graded Plates and Shells*, Vietnam National University Press, Hanoi.

Duc, N.D. (2014b), "Nonlinear dynamic response of imperfect eccentrically stiffened FGM double curved shallow shells on elastic foundation", *J. Compos. Struct.*, **102**, 306-314. https://doi.org/10.1016/j.compstruct.2012.11.017.

Duc, N.D. (2016), "Nonlinear thermal dynamic analysis of eccentrically stiffened S-FGM circular cylindrical shells surrounded on elastic foundations using the Reddy's third-order shear deformation shell theory", *Eur. J. Mech. A/Solid.*, **58**, 10-30. https://doi.org/10.1016/j.euromechsol.2016.01.004.

Duc, N.D. and Minh, D.K. (2010), "Bending analysis of three-phase polymer composite plates reinforced by glass fibers and Titanium oxide particles", *J. Comput. Mater. Sci.*, **49**, 194-198. https://doi.org/10.1016/j.commatsci.2010.04.016.

Duc, N.D., Hadavinia, H., Thu, P.V. and Quan, T.Q. (2015), "Vibration and nonlinear dynamic response of imperfect three-phase polymer nanocomposite panel resting on elastic foundations under hydrodynamic loads", *Compos. Struct.*, **131**, 229-237. https://doi.org/10.1016/j.compstruct.2015.05.009.

Duc, N.D., Khoa, N.D. and Thiem, H.T. (2018), "Nonlinear thermo-mechanical response of eccentrically stiffened Sigmoid FGM circular cylindrical shells subjected to compressive and uniform radial loads using the Reddy's third-order shear deformation shell theory", *Mech. Adv. Mat. Struct.*, **25**, 1157-1167. https://doi.org/10.1080/15376494.2017.1341581.

Duc, N.D., Quan, T.Q. and Nam, D. (2013), "Nonlinear stability analysis of imperfect three phase polymer composite plates", *J. Mech. Compos. Mater.*, **49**, 345-358. ttps://doi.org/10.1007/s11029-013-9352-4.

Frikha, A., Hajlaoui, A., Wali, M. and Dammak, F. (2016), "A new higher order C0 mixed beam element for FGM beams analysis", *Compos. Part B.*, **106**, 181-189. https://doi.org/10.1016/j.compositesb.2016.09.024.

Ghavanloo, E. and Fazelzadeh, A. (2011), "Flow-thermoelastic vibration and instability analysis of viscoelastic carbon nanotubes embedded in viscous fluid", *Physica E.*, **44**, 17-24. https://doi.org/10.1016/j.physe.2011.06.024.

GhorbanpourArani, A., Bagheri, M.R., Kolahchi, R. and KhodamiMaraghi, Z. (2013), "Nonlinear vibration and instability of fluid-conveying DWBNNT embedded in a visco-

Pasternak medium using modified couple stress theory", *J. Mech. Sci. Tech*., **27**(9), 2645-2658. https://doi.org/10.1007/s12206-013-0709-3.

Gong, S.W., Lam, K.Y. and Lu, C. (2000), "Structural analysis of a submarine pipeline subjected to underwater shock", *Int. J. Pres. Ves. Pip*., **77**, 417-423. https://doi.org/10.1016/S0308-0161(00)00022-3.

Hajlaoui, A., Chebbi, E., Wali, M. and Dammak, F. (2019a), "Geometrically nonlinear analysis of FGM shells using solid-shell element with parabolic shear strain distribution", *Int. J. Mech. Mater. Des.*, 1-16. https://doi.org/10.1007/s10999-019-09465-x.

Hajlaoui, A., Chebbi, E., Wali, M. and Dammak, F. (2019b), "Buckling analysis of carbon nanotube reinforced FG shells using an efficient solid-shell element based on a modified FSDT", *Thin Wall. Struct*., **144**, 106254. https://doi.org/10.1016/j.tws.2019.106254.

Hajlaoui, A., Chebbi, E., Wali, M. and Dammak, F. (2019c), "Static analysis of carbon nanotube-reinforced FG shells using an efficient solid-shell element with parabolic transverse shear strain", *Eng. Comput*. https://doi.org/10.1108/EC-02-2019-0075.

Hajlaoui, A., Triki, E., Frikha, A., Wali, M. and Dammak, F. (2017), "Nonlinear dynamics analysis of FGM shell structures with a higher order shear strain enhanced solid-shell element", *Latin. Am. J. Solid. Struct.*, **14**, 72-91. http://dx.doi.org/10.1590/1679-78253323.

Housner, G.W. (1952), "Bending vibrations of a pipe line containing flowing fluid", *J. Appl. Mech.*, **19**, 205-208.

Huang, Y.M., Liu, Y.S., Li, B.H., Li, Y.J. and Yue, Z.F. (2010), "Natural frequency analysis of fluid conveying pipeline with different boundary conditions", *Nucl. Eng. Des*., **240**(3), 461-467. https://doi.org/10.1016/j.nucengdes.2009.11.038.

Inozemtcev, A.S., Korolev, E.V. and Smirnov, V.A. (2017), "Nanoscale modifier as an adhesive for hollow microspheres to increase the strength of high-strength lightweight", *Struct.*, **18**(1), 67-74. https://doi.org/10.1002/suco.201500048.

JafarianArani, A and Kolahchi, R. (2016), "Buckling Analysis of embedded columns armed with carbon nanotubes", *Comput. Concrete*, **17**(5), 567-578. https://doi.org/10.12989/cac.2016.17.5.567.

Kim, D.H., Lee, G.N., Lee, Y. and Lee, I.K. (2015), "Dynamic reliability analysis of offshore wind turbine support structure under earthquake", *Wind Struct*., **21**, 609-623. https://doi.org/10.12989/was.2015.21.6.609.

Kolahchi, R., RabaniBidgoli, M., Beygipoor, G.H. and Fakhar, M.H. (2015), "A nonlocal nonlinear analysis for buckling in embedded FG-SWCNT-reinforced microplates subjected to magnetic field", *J. Mech. Sci. Tech*., **29**, 3669-3677. https://doi.org/10.1007/s12206-015-0811-9.

Lam, K.Y., Zong, Z. and Wang, Q.X. (2003), "Dynamic response of a laminated pipeline on the seabed subjected to underwater shock", *Compos. Part B-Eng*., **34**, 59-66. https://doi.org/10.1016/S1359-8368(02)00072-0.

Lee, U. and Oh, H. (2003), "The spectral element model for pipelines conveying internal steady flow", *Eng. Struct*., **25**, 1045-1055. https://doi.org/10.1016/S0141-0296(03)00047-6.

Lin, W. and Qiao, N. (2008), "Vibration and stability of an axially moving beam immersed in fluid", *Int. J. Solid. Struct*., **45**, 1445-1457. https://doi.org/10.1016/j.ijsolstr.2007.10.015.

Liu, X., Zhang, H., Gu X., Chen, Y., Xia, M. and Wu, K. (2017), "Strain demand prediction method for buried X80 steel pipelines crossing oblique-reverse faults", *Earthq. Struct*., **12**, 321-332. https://doi.org/10.12989/eas.2017.12.3.321.

Liu, Z.G., Liu, Y. and Lu, J. (2012), "Fluid-structure interaction of single flexible cylinder in axial flow", *Comput. Fluid.*, **56**, 143-151. https://doi.org/10.1016/j.compfluid.2011.12.003.

Mohammadian, H., Kolahchi, R. and Rabani Bidgoli, M. (2017), "Dynamic response of beams reinforced by Fe_2O_3 nanoparticles subjected to magnetic field and earthquake load", *Earthq. Struct*., **13**, 589-598. https://doi.org/10.12989/eas.2017.13.6.589.

Mori, T. and Tanaka, K. (1973), "Average stress in matrix and average elastic energy of materials with misfitting inclusions", *Acta. Metall. Mater*., **21**, 571-574. https://doi.org/10.1016/0001-6160(73)90064-3.

Motezaker, M. and Kolahchi, R. (2017), "Seismic response of CNT nanoparticles-reinforced pipes based on DQ and newmark methods", *Comput. Concrete*, **19**(6), 745-753. https://doi.org/10.12989/cac.2017.19.6.745.

Nogueira, A.C. (2012), "Rationally modeling collapse due to bending and external pressure in pipelines", *Earthq. Struct.*, **3**, 473-494. https://doi.org/10.12989/eas.2012.3.3_4.473.

Paidoussis, M.P. and Issid, N.T. (1974), "Dynamic stability of pipes conveying fluid", *J. Sound Vib*., **33**, 267-294. https://doi.org/10.1016/S0022-460X(74)80002-7.

RabaniBidgoli, M. and Saeidifar, M. (2017), "Time-dependent buckling analysis of CNT nanoparticles reinforced columns exposed to fire", *Comput. Concrete*, **20**(2), 119-127. https://doi.org/10.12989/cac.2017.20.2.119.

RabaniBidgoli, M., Karimi, M.S. and GhorbanpourArani, A. (2016), "Nonlinear vibration and instability analysis of functionally graded CNT-reinforced cylindrical shells conveying viscous fluid resting on orthotropic Pasternak medium", *Mech. Adv. Mater. Struct*., **23**(7), 819-831. https://doi.org/10.1080/15376494.2015.1029170.

Ray, M.C. and Reddy, J.N. (2013), "Active damping of laminated cylindrical shells conveying fluid using 1-3 piezoelectric composites", *Compos. Struct*., **98**, 261-271. https://doi.org/10.1016/j.compstruct.2012.09.051.

Safari Bilouei, B., Kolahchi, R. and Rabanibidgoli, M. (2016), "Buckling of columns retrofitted with Nano-Fiber Reinforced Polymer (NFRP)", *Comput. Concrete*, **18**(5), 1053-1063. https://doi.org/10.12989/cac.2016.18.5.1053.

Shamsuddoha, M., Islam, M.M., Aravinthan, T., Manalo, A. and Lau, K.T. (2013), "Effectiveness of using fibre-reinforced polymer composites for underwater steel pipeline repairs", *Compos. Struct*., **100**, 40-54. https://doi.org/10.1016/j.compstruct.2012.12.019.

Sharifi, M., Kolahchi, R. and Rabani Bidgoli, M. (2018), "Dynamic analysis of beams reinforced with Tio_2 nano particles under earthquake load", *Wind Struct*., **26**, 1-9. https://doi.org/10.12989/was.2018.26.1.001.

Shokravi, M. (2017), "Vibration analysis of silica nanoparticles-reinforced beams considering agglomeration effects", *Comput. Concrete*, **19**(3), 333-338. https://doi.org/10.12989/cac.2017.19.3.333.

Simsek, M. (2010), "Non-linear vibration analysis of a functionally graded Timoshenko beam under action of a moving harmonic load", *Compos. Struct*., **92**, 2532-2546. https://doi.org/10.1016/j.compstruct.2010.02.008.

Su, Y., Li, J., Wu, C and Li, Z.X. (2016), "Influences of nano-particles on dynamic strength of ultra-high performance", *Compos. Part B-Eng*., **91**, 595-609. https://doi.org/10.1016/j.compositesb.2016.01.044.

Thinh, T.I. and Nguyen, M.C. (2016), "Dynamic stiffness method for free vibration of composite cylindrical shells containing fluid", *Appl. Math. Model*., **40**, 9286-9301. https://doi.org/10.1016/j.apm.2016.06.015.

Yoon, H.I. and Son, I. (2007), "Dynamic response of rotating flexible cantilever fluid with tip mass", *Int. J. Mech. Sci*., **49**, 878-887. https://doi.org/10.1016/j.ijmecsci.2006.11.006.

ZamaniNouri, A. (2017), "Mathematical modeling of pipes reinforced with CNTs conveying fluid for vibration and stability analyses", *Comput. Concrete*, **19**(3), 325-331.

https://doi.org/10.12989/cac.2017.19.3.325.
Zhai, H., Wu, Z., Liu, Y. and Yue, Z. (2011), "Dynamic response of pipeline conveying fluid to random excitation", *Nucl. Eng. Des*., **241**, 2744-2749. https://doi.org/10.1016/j.nucengdes.2011.06.024.
Zhou, X.Q., YU, D.Y., Shao, X.Y., Zhang, C.Y. and Wang, S. (2017), "Dynamics characteristic of steady fluid conveying in the periodical partially viscoelastic composite pipeline", *Compos. Part B-Eng*., **111**, 387-408. https://doi.org/10.1016/j.compositesb.2016.11.059.

CC